Line strengths of rovibrational and rotational transitions within the X 3   ground state of NH

James S. A. Brooke, Peter F. Bernath, Colin M. Western, Marc C. van Hemert, and Gerrit C. Groenenboom

Line strengths of rovibrational and rotational transitions within the $X^3\Sigma^-$ ground state of NH

James S. A. Brooke,[1,a)] Peter F. Bernath,[1,2] Colin M. Western,[3] Marc C. van Hemert,[4] and Gerrit C. Groenenboom[5]

[1]*Department of Chemistry, University of York, York YO10 5DD, United Kingdom*
[2]*Department of Chemistry and Biochemistry, Old Dominion University, 4541 Hampton Boulevard, Norfolk, Virginia 23529-0126, USA*
[3]*School of Chemistry, University of Bristol, Cantock's Close, Bristol BS8 1TS, United Kingdom*
[4]*Faculty of Science, Leiden Institute of Chemistry, Theoretical Chemistry, Gorlaeus Laboratories, Einsteinweg 55, 2333 CC Leiden, The Netherlands*
[5]*Theoretical Chemistry, Institute for Molecules and Materials (IMM), Radboud University Nijmegen, Heyendaalseweg 135, 6525 AJ Nijmegen, The Netherlands*

A new line list for rovibrational and rotational transitions, including fine structure, within the NH $X^3\Sigma^-$ ground state has been created. It contains line intensities in the form of Einstein A and f-values, for all possible bands up to $v' = 6$, and for J up to between 25 and 44. The intensities are based on a new dipole moment function (DMF), which has been calculated using the internally contracted multi-reference configuration interaction method with an aug-cc-pV6Z basis set. The programs RKR1, LEVEL, and PGOPHER were used to calculate line positions and intensities using the most recent spectroscopic line position observations and the new DMF, including the rotational dependence on the matrix elements. The Hund's case (b) matrix elements from the LEVEL output (available as Supplement 1 of the supplementary material) have been transformed to the case (a) form required by PGOPHER. New relative intensities for the (1,0) band have been measured, and the calculated and observed Herman-Wallis effects are compared, showing good agreement. The line list (see Supplement 5 of the supplementary material) will be useful for the study of NH in astronomy, cold and ultracold molecular systems, and in the nitrogen chemistry of combustion. © 2014 AIP Publishing LLC. [http://dx.doi.org/10.1063/1.4891468]

I. INTRODUCTION

In astronomy and in general for remote sensing, lists of line positions and absolute line intensities are essential for the determination of molecular abundances.[1,2] A combination of laboratory measurements of molecules and theoretical methods can be used effectively in the creation of such line lists.[2]

Imidogen (NH) is an important molecule in the study of astronomical environments, as it is present in cool stars,[3–6] comets,[7] diffuse interstellar clouds,[8–11] and the Sun.[12–16] It has also been magnetically trapped at temperatures less than 1 K,[17–20] and there is potential for trapping[21–24] and chemical reactions[25] at ultracold temperatures (<1 mK),[26–28] applications for which include high precision spectroscopy[26,29] and quantum computing.[30] NH is also important in the nitrogen chemistry that occurs in combustion processes,[31,32] and is a key species in the transformation of N_2 to NH_3 (and vice versa) in stellar and exoplanet atmospheres.[33,34]

The vibration-rotation (V-R) transitions within the $X^3\Sigma^-$ ground state are the focus of this paper, and their importance is illustrated by the fact that as well being used to calculate NH abundance, they have been used to calculate the total nitrogen abundance in cool stars[4–6,35] and the Sun.[14,36] The CN

molecule has also been used for this purpose[36] but it is less useful as the spectroscopic knowledge has been less complete, although this situation has recently been improved.[37]

The first observations of these transitions were of the 1-0 band by Bernath and Amano in 1982.[38] In 1986, Boudjaadar *et al.* observed the $\Delta v = 1$ sequence up to the 5-4 band,[39] and transitions in these bands were detected for a greater number of N values by Ram *et al.* in 1999,[40] at the National Solar Observatory at Kitt Peak, Arizona. Ram and Bernath reported additional lines in these bands in 2010,[41] and also transitions in the previously unobserved 6-5 band. In 1989, Chackerian *et al.*[42] studied the relative intensities of the lines recorded by Boudjaadar *et al.*[39]

Pure rotational transitions were first seen in 1975 by Radford and Litvak,[43] who observed only the $N = 1-0$ transition in the $v = 0$ level. Wayne and Radford then detected more rotational transitions within both $v = 0$ and 1 in 1976.[44] In 1982, van den Heuvel *et al.*[45] reported more observations of the $v = 0$, $N = 1-0$ transition, but higher N transitions remained undetected. Solar spectra recorded in space by the ATMOS Fourier Transform Spectrometer[15] (FTS; part of Spacelab 3 onboard some Space Shuttle flights) provided infrared rotational lines between 600 and 900 cm^{-1}, covering $N'' = 20$-35 in $v = 0$, and $N'' = 21$-29 in $v = 1$. Similar solar spectra taken by ACE (Atmospheric Chemistry Experiment),[46,47] also from low Earth orbit, provided higher N rotational lines; up to N''

a)jsabrooke@gmail.com

TABLE I. Summary of equilibrium dipole moments, μ_e, and v = 0 averaged dipole moments, μ_0, for the $X^3\Sigma^-$ ground state of NH, since 1974. All but Paldus and Li (1996)[62] and the experimental study calculated full dipole moment functions. Our calculated values are also included.

Year	Authors	μ_e (debye)	μ_0 (debye)
1974	Scarl and Dalby[52] (expt.)	1.405 ± 0.077^a	1.389 ± 0.075
1974	Das *et al.*[56]	1.5353^b	1.5155^b
1975	Meyer and Rosmus[57]	1.578	1.5546^b
1976	Hay and Dunning[58]	1.526	…
1987	Goldfield and Kirby[59]	1.511	1.480
1992	Stallcop *et al.*[60]	1.530	…
1992	Cantarella *et al.*[61]	1.5054	1.4827
1996	Paldus and Li[62]	1.536	…
2014	Campbell *et al.*[19]/This work	1.5434	1.5246

^{a}Calculated by Chackerian *et al.*[42,53] using the reported data of Scarl and Dalby.[52]
^{b}Calculated by Cantarella *et al.*[61] using the reported data of Das *et al.*[56] or Meyer and Rosmus.[57]

= 42 in v = 0. More recent laboratory measurements of lower N rotational transitions have been made for v = 0 by Klaus *et al.*[48] in 1997 (N = 1-0), Lewen *et al.*[49] in 2004 (N = 2-1), and Flores-Mijangos *et al.*[50] (up to N = 5-4). In 2007, Robinson *et al.*[51] observed transitions up to N = 5-4 in v = 1, and also for the first time in v = 2 (up to N = 5-4).

The most recent set of molecular constants for the $X^3\Sigma^-$ state were reported by Ram and Bernath in 2010.[41] Their calculations used V-R lines from Ram *et al.*,[40] Geller *et al.*,[15] Bernath and Amano,[38] spectra from the ACE mission,[47] and their new 6-5 band observations reported in that paper. They used pure rotational lines from Robinson *et al.*,[51] Flores-Mijangos *et al.*,[50] Lewen *et al.*,[49] Klaus *et al.*,[48] Geller *et al.*,[15] and the ATMOS instrument.[15] They performed a line position fit to provide updated molecular constants for vibrational levels up to v = 6.

An experimental average ground state dipole moment, μ_0, of 1.389 ± 0.07 D was obtained in 1974 by Scarl and Dalby.[52] They compared it to theoretical dipole moments available at the time, which varied widely between 0.36 and 2.17 D. Dipole moments and dipole moment functions (DMFs) have been calculated several times since then using various theoretical methods, and a summary of such studies showing their resulting values of μ_e and μ_0 is shown in Table I. Using μ_e as a comparison, there is still some disagreement between these values, and all of them are somewhat higher than the experimental value of μ_e = 1.405 ± 0.077.[42,52,53] The difference between the full DMFs is more complicated than this of course (see Sec. III D for an example). Values for μ_e are compared in Table I as they are readily available in the literature and give an indication of the quality of the calculations. However, it is actually the first derivative of the dipole moment that has the greatest effect on the lifetime and line intensities of rovibrational transitions. More recent theoretical studies of NH include those of Feller and Sordo[54] and Temelso *et al.*,[55] in which high levels of theory were used to calculate potential energy curves and spectroscopic constants, but no DMFs were reported.

Currently available line intensities in the JPL[63] and CDMS[64,65] spectroscopic databases are based on the dipole moment from 1974 of Scarl and Dalby.[52] These line intensities are still being used, for example, by Goicoechea *et al.*[10] Grevesse *et al.*[14,36] calculated the nitrogen abundance in the Sun, and they used the 1975 DMF of Meyer and Rosmus[57] to calculate their own line intensities. Aoki and Tsuji[6] also used this DMF in their calculations of N abundance in oxygen-rich giants. A new DMF would be useful to resolve the above discrepancies and calculate a new set of line intensities.

In 2008, Campbell *et al.*[19] magnetically trapped NH to obtain an accurate experimental vibrational lifetime for v = 1 of $37.0 \pm 0.5_{\mathrm{stat}}{}^{+2.0}_{-0.8\mathrm{syst}}$ ms. They found disagreement with the previous values of Dodd *et al.*,[66] who used the DMF of Goldfield and Kirby[59] to calculate $A_{10} = 51.7$ s^{-1} ($\tau_{v=1}$ = 19.3 ms), and with Rosmus and Werner[67] who gave A_{10} = 34.9 s^{-1} ($\tau_{v=1}$ = 28.7 ms). To compare their experimental result to theory, they calculated a new DMF using the multi-reference configuration interaction (MRCI) method with an aug-cc-pV6Z basis set. The resulting lifetime of 36.99 ms is an excellent match to their experimental lifetime. They calculated a value of μ_0 of 1.5246 D. The DMF itself was not published, and the purpose of this paper is to use this DMF and the positions from Ram and Bernath[41] to create a new line list for the NH $X^3\Sigma^-$ state rovibrational transitions, complete with positions and absolute intensities. The range of the DMF has been extended for this study to 0.6-20 a_0 (0.32-10.6 Å)

II. CALCULATION OF LINE INTENSITIES

A. Overview

The rovibrational levels of the NH $X^3\Sigma^-$ state are labeled not only by their total angular momentum quantum number J and vibrational quantum number v, but also by F_1, F_2, and F_3 for the three fine structure levels arising from interaction of the spin angular momentum ($S = 1$) with the nuclear rotational angular momentum (quantum number N). For F_1, $N = J - S$, for F_2, $N = J$, and for F_3, $N = J + S$. In the following equations we use η to represent all quantum numbers apart from J.

The rotational line intensities reported in this paper are in the form of Einstein A values, which are also converted to absorption oscillator strengths (f-values), using the equation[68]

$$f_{\eta'J' \leftarrow \eta J} = \frac{m_e \epsilon_0 c^3}{2\pi e^2 \nu^2} \frac{(2J'+1)}{(2J+1)} A_{\eta'J' \rightarrow \eta J} \tag{1}$$

$$= 1.4991937827 \frac{1}{\tilde{\nu}^2} \frac{(2J'+1)}{(2J+1)} A_{\eta'J' \rightarrow \eta J}, \tag{2}$$

where $A_{\eta'J' \rightarrow \eta J}$ and ν are in s^{-1}, and $\tilde{\nu}$ is in cm^{-1}. Western's PGOPHER[69] is used to calculate Einstein A values with the equation

$$A_{\eta'J' \rightarrow \eta J} = \frac{16\pi^3 \nu^3 S_{\eta'J'\eta J}}{3\epsilon_0 hc^3 (2J'+1)} \tag{3}$$

$$= 3.13618932 \times 10^{-7} \frac{\tilde{\nu}^3 S_{\eta'J'\eta J}}{(2J'+1)}, \tag{4}$$

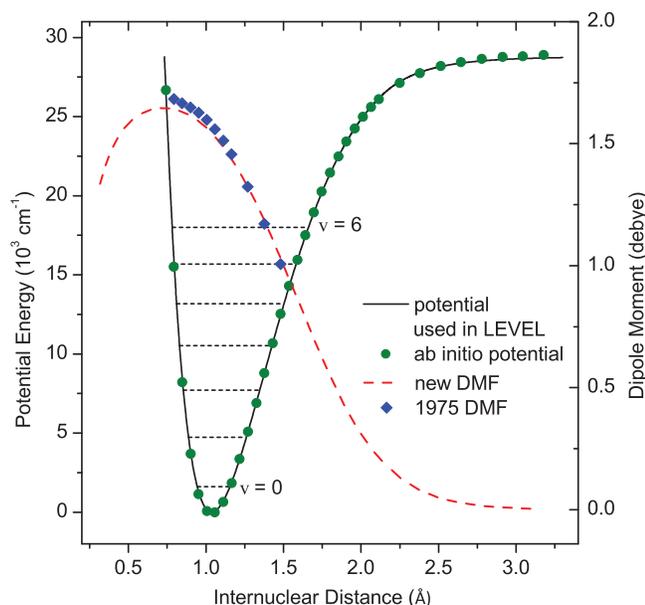where the line strength, $S_{\eta'J'\eta J}$, is in debye squared.

FIG. 1. Calculated potential energy curves and DMFs for the $X^3\Sigma^-$ ground state of NH. The black line is the potential used in LEVEL, and the green circles are the *ab initio* potential (calculated along with the DMF and reported by Campbell *et al.*[19]). The red dashed line is the DMF used in this study (reported by Campbell *et al.*[19]), and the blue diamonds are the DMF calculated by Meyer and Rosmus.[57]

TABLE II. Equilibrium molecular constants for the NH $X^3\Sigma^-$ state.

Constant[a]	Value
ω_e	3282.220(15)[b]
$\omega_e x_e$	78.513(15)
$\omega_e y_e$	0.1341(61)
$\omega_e z_e$	$-0.0066(11)$
$\omega_e \eta_e$	$-0.003141(70)$
B_e	16.667704(29)
α_{e_1}	0.649670(91)
α_{e_2}	0.001674(71)
α_{e_3}	$-0.000067(25)$
α_{e_4}	$-0.0000633(24)$

[a]These constants are the usual power series expansions in v + 1/2, with negative signs in front of $\omega_e x_e$ and α_{e_1}.

[b]Numbers in parentheses indicate one standard deviation to the last significant digits of the constants.

Le Roy's LEVEL[70] program calculates rovibrational wavefunctions by solving the 1D Schrödinger equation, with the input of a potential energy curve. It then uses these and a specified DMF to calculate transition dipole moment matrix elements (TDMMEs), which, as LEVEL does not include spin, are the matrix elements (MEs) of the DMF in a pure rovibrational basis. These are referred to as Hund's case (b) TDMMEs, and they are available in Supplement 1 of the supplementary material.[71] They are transformed into the case (a) TDMMEs required by PGOPHER, from which values for $S_{\eta'J'\eta J}$ and $A_{\eta'J'\to\eta J}$ are obtained, through a series of steps. For details of the calculation of $S_{\eta'J'\eta J}$ from the case (b) TDMMEs, please see both sections of the Appendix.

The DMF used here was calculated previously and used in the calculations of Campbell *et al.*,[19] but not reported. Its calculation is described in Sec. II B, and it is shown in Table III and Figure 1.

The potential energy curve for the NH $X^3\Sigma^-$ state is calculated here with Le Roy's RKR1[72] program, which uses the first-order semiclassical Rydberg-Klein-Rees procedure[73–76](the final potential used in LEVEL is available in Supplement 2 of the supplementary material[71]). This requires the input of molecular equilibrium constants, which were calculated from the molecular constants of Ram and Bernath,[41] and those used are shown in Table II. The calculated potential curve is shown along with the DMF in Figure 1. A dissociation energy of 27 176 cm^{-1} was taken from Espinosa-Garcia *et al.*[77] for extrapolation of the potential energy curve at long range.

Line positions were also calculated with PGOPHER, which uses the standard N^2 Hamiltonian for a $^3\Sigma^-$ state, and the molecular constants were taken directly from Ram and Bernath.[41] The Hamiltonian MEs used are listed in the online documentation of PGOPHER, and the explicit MEs used in this study are the same as those previously listed by Brazier *et al.*[78]

B. Calculation of the new dipole moment function

The calculation of the DMF was previously described by Campbell *et al.*,[19] and will be briefly explained here. It was calculated as expectation values with the *ab initio* internally contracted MRCI method,[79,80] using MOLPRO 2006.1,[81] and a large aug-cc-pV6Z one electron basis set[82–84] was employed. The molecular orbitals were calculated at the complete active space self consistent field (CASSCF) level. The C_{2v} point group symmetry was used, and the active space consisted of the 1-$6a_1$, 1-$3b_1$, 1-$3b_2$, and 1-$2a_2$ orbitals. All CASSCF configurations were used as reference configurations in the MRCI step.

In Campbell *et al.*, the DMF used had been calculated for internuclear distances between 1.0 and 3.0 a_0 (0.53 to 1.59 Å). In order to be able to accurately calculate TDMMEs for vibrational levels up to v = 6 and J = 40, this range was later extended to 0.6-20 a_0 (0.32-10.6 Å). The calculated DMF is shown in Table III (converted from atomic units using 1 D = 0.39343031369 ea_0 and 1 Å = 1.88972612 a_0, and is available in Supplement 3 of the supplementary material[71] along with the calculated *ab initio* potential (in atomic units).

At an internuclear distance of $R \approx 10$ Å the dipole moment is about -0.00165 D. At the CASSCF level, the dipole moment at this distance is about an order of magnitude larger. We conclude that this residual dipole moment is an artifact of the truncation of the active space, which is only partly corrected at the internally contracted MRCI step of the calculation. The residual dipole is small compared to the equilibrium value and changing the DMF by a constant does not affect the calculated line strengths. Furthermore, the amplitudes of the vibrational wave functions for $R > 5.25$ Å are smaller than 10^{-5}, so we decided not to attempt to correct the long range behavior of the DMF.

We believe that our *ab initio* DMF is the most accurate DMF available, based on arguments provided by Campbell *et al.*[19] In the MRCI calculations, the DMF was used to

TABLE III. Calculated dipole moment function for the NH $X^3\Sigma^-$ state.

r (Å)	μ (D)	r (Å)	μ (D)
0.31750633	1.33547488	1.64044935	0.78544598
0.34396519	1.39367433	1.69336708	0.70420372
0.37042405	1.44198960	1.74628480	0.62540407
0.39688291	1.48209917	1.79920252	0.55002503
0.42334177	1.51540207	1.85212024	0.47892878
0.44980063	1.54304783	1.90503796	0.41323669
0.47625949	1.56597458	1.95795568	0.35342338
0.50271835	1.58494170	2.01087340	0.29967584
0.52917721	1.60053915	2.06379112	0.25227372
0.58209493	1.62355141	2.11670884	0.21089732
0.63501265	1.63787893	2.24900315	0.13112447
0.68793037	1.64520599	2.38129745	0.07877570
0.74084810	1.64641330	2.51359175	0.04682247
0.79376582	1.64187747	2.64588606	0.02783687
0.84668354	1.63161556	2.77818036	0.01644904
0.89960126	1.61544649	2.91047466	0.00958660
0.95251898	1.59312483	3.04276896	0.00541524
1.00543670	1.56441623	3.17506327	0.00284421
1.05835442	1.52913964	3.43965187	0.00029543
1.11127214	1.48723095	3.70424048	− 0.00073901
1.16418986	1.43871888	3.96882908	− 0.00127003
1.21710759	1.38382496	4.23341769	− 0.00145136
1.27002531	1.32291100	4.76259490	− 0.00164245
1.32294303	1.25646147	5.29177211	− 0.00169789
1.37586075	1.18496853	6.35012653	− 0.00170170
1.42877847	1.10952353	7.40848095	− 0.00168396
1.48169619	1.03082967	8.46683538	− 0.00166784
1.53461391	0.94988204	9.52518980	− 0.00165816
1.58753163	0.86774152	10.58354422	− 0.00165069

FIG. 2. Effect of rotation on the vibrational wavefunctions of the $d^3\Pi_g$, v = 4 state of C_2 and the $X^3\Sigma^-$, v = 4 state of NH (v = 4 levels chosen arbitrarily as examples).

compute the radiative lifetime of the v = 1 vibrational state of NH, and the result was 36.99 ms, in perfect agreement with the experimental value of 37.0 ± 0.5 ms determined in the same study. It was also shown that a DMF computed with another high-level *ab initio* method, the RCCSD(T) method, gave very similar results and that the dipole moment of the v = 0 state computed with the MRCI DMF is in good agreement with the high level *ab initio* calculation of Paldus and Li.[62]

C. The Herman-Wallis effect

The rotation of a diatomic molecule results in a centrifugal force, which displaces the atoms and increases the bond length.[85] This causes the vibrational wavefunctions to change with different amounts of rotation, which therefore means that the TDMMEs depend on rotation. This is called the Herman-Wallis (H-W) effect. Also, as has been shown before by Chackerian *et al.*[42] (see their Eq. (3)), the sign and magnitude of the Herman-Wallis effect mainly depends on the dipole moment and its first derivative with respect to the internuclear distance.

Calculations of the type reported in this paper often use one rotationless TDMME for a vibrational band, and the effect of rotation on the vibrational wavefunction is ig-
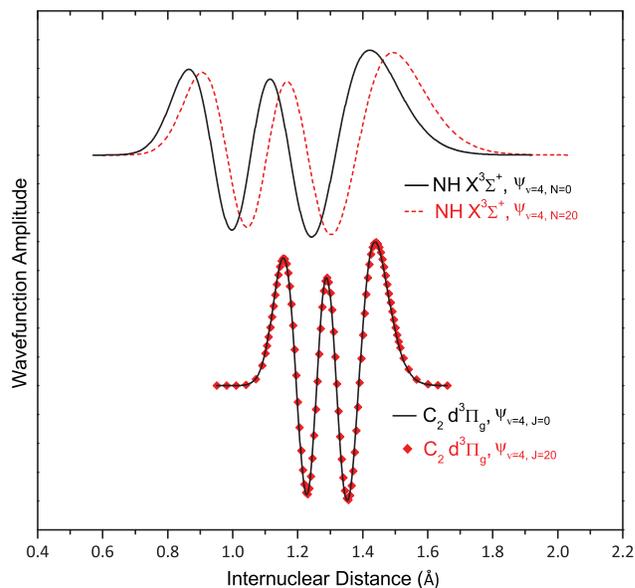
nored. This can be a very good approximation for molecules with heavier atoms, but NH contains a light H atom which is strongly affected by the centrifugal force. An illustration of the magnitude of the H-W effect in NH is shown in Figure 2, which shows how the vibrational part of the wavefunction changes with N and J for NH and C_2. Although the effect is quite small with heavier atoms, if transitions in vibrational bands with a small Franck-Condon factor in an electronic transition are being calculated, it can still be noticeable.[37, 86, 87]

We have included the H-W effect in these calculations by calculating TDMMEs for the full range of J values that are intended to be reported, and then entering the individual MEs into PGOPHER (one for each $J'\Omega' - J''\Omega''$ transition; see also Sec. I).

III. RESULTS AND DISCUSSION

A. New NH FTS spectrum

To validate the results it is useful to compare the relative intensities of a calculated spectrum with an observed spectrum, as the measurement of absolute intensities is extremely difficult. The H-W effect has a major impact on the spectrum, with a decrease in intensity of the P branches relative to the R branches. To see if the inclusion of the H-W effect has been done correctly, the intensities need to be compared over a large enough wavenumber range to cover both branches. The spectrum observed by Ram and Bernath[41] would probably suffice for this purpose, but its *y*-axis had not been calibrated for the instrument response, and so the intensity may drift over the wavenumber range observed.

A new spectrum was recorded at Old Dominion University, Norfolk, VA, USA, with the aim of providing relative intensities that are calibrated across the full wavenumber range.
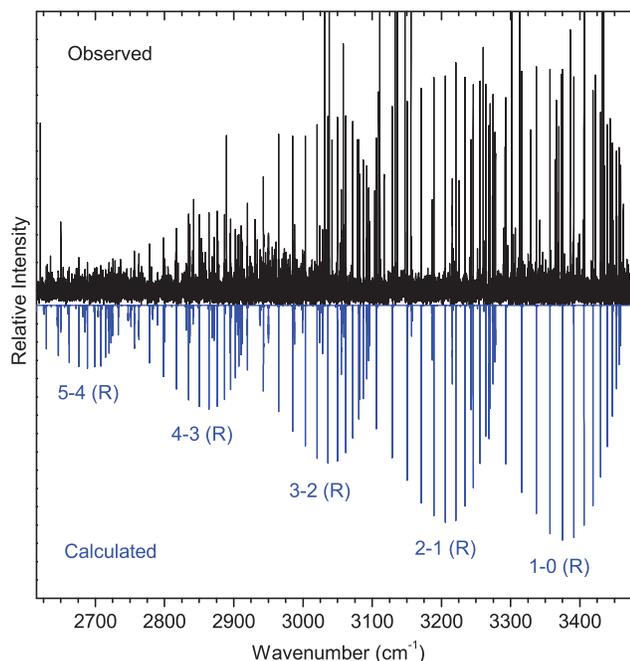
FIG. 3. Observed and calculated spectra of NH. The lines that continue past the top of the *y*-axis are intense atomic lines. The features that can clearly be seen are the R branches of the 1-0, 2-1, 3-2, 4-3, and 5-4 bands. The calculated spectrum was convolved with a Gaussian function to best match the observed broadening. Effective rotational and vibrational temperatures of 1800 K and 5000 K were used, respectively.
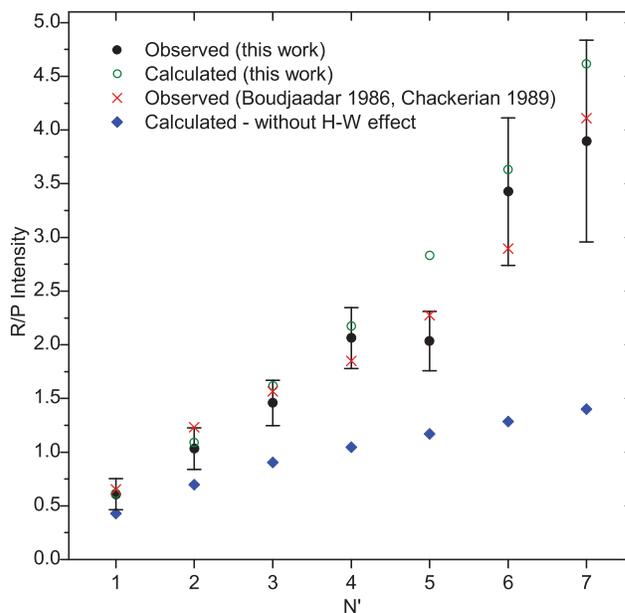

FIG. 4. Ratio of P and R branch relative intensities, for the new observed spectrum, the calculated spectrum, the spectrum observed by Boudjaadar *et al.*[39] and analyzed by Chackerian *et al.*,[42] and the calculated spectrum without the inclusion of the Herman-Wallis effect. The error bars are large for the higher N' values due to the low signal to noise ratio observed in the P branch. A good match is seen between both sets of observed values and the calculated values including the H-W effect, except for $N' = 5$ from the spectrum observed in this work. This could be due to a line overlapping the $^P P_3(6)$ line as this appears more intense than expected.

NH was created in a microwave discharge of a mixture of N_2 (0.8 Torr), H_2 (0.3 Torr), and He (0.9 Torr). The emission spectrum was recorded with a Bruker IFS 125 HR FTS, using a CaF_2 beam splitter and a liquid nitrogen cooled InSb detector. Data were recorded between 1800 and 5000 cm^{-1}, limited by the InSb detector and a Ge filter. As intensities but not line positions were important, a relatively low resolution of 0.04 cm^{-1} was used to improve the signal-to-noise ratio, and 688 scans were coadded to give the uncalibrated spectrum. Immediately afterwards, the discharge cell was replaced by a 1256 K blackbody, and 144 scans were coadded under the same conditions. The instrument function was corrected for by dividing the NH spectrum by the blackbody spectrum and the baseline was then subtracted to give the final spectrum.

The relevant wavenumber range is shown along with the calculated spectrum in Figure 3, and a good match is seen. The calculated spectrum was convolved with a Gaussian function to best match the observed broadening, and rotational and vibrational temperatures of 1800 K and 5000 K, respectively, were found to give the closest match. In the microwave discharge, energy transfer between the excited gases and various vibrational and rotational levels of the NH molecules will occur, resulting in level populations that are not in thermodynamic equilibrium. This means that specifying separate rotational and vibrational temperatures provides only an approximate model for the spectrum. This also explains why the two temperatures are very different, and why, as can be seen in Figures 3 and 5, the intensity within the R branch decreases more quickly with increasing wavenumber in the calculated

spectrum than in the observed spectrum. However, this is not an issue when comparing the H-W effect, as explained in Sec. III B.

B. Spectral validation

In checking that the H-W effect has been applied correctly, it is the difference in intensity between the R and P branch that is most important. To quantify this, the observed and calculated intensities in the 1-0 band were compared for as many N' levels as were available in both branches. For each observed N' level, the peak heights of the F_1-F_1, F_2-F_2, and F_3-F_3 lines (where available) were summed for the R and P branches separately, and the R branch total was divided by the P branch total, giving the R/P ratio. The same was done for the calculated spectrum, using exactly the same peaks (the intensities vary with temperature, but the R/P ratio does not). The results are shown in Figure 4. The inclusion of the H-W effect is clearly an improvement. This improvement is also seen in Figure 5, where the spectrum calculated (using the conditions described in Sec. III A) using the H-W effect clearly better matches the difference between R and P branch intensity in the observed spectrum.

Observed intensities were also obtained from Chackerian *et al.*,[42] who analyzed the spectra observed by Boudjaadar *et al.*[39] They reported reduced intensities, in the form $\ln(6.23 \times 10^{23} \times S^{\Delta J}_{J''} I \tilde{\nu}^4)$, where $S^{\Delta J}_{J''}$ is the Hönl-London factor, and I is the required observed intensity. They described how they calculated their Hönl-London factors, and so values
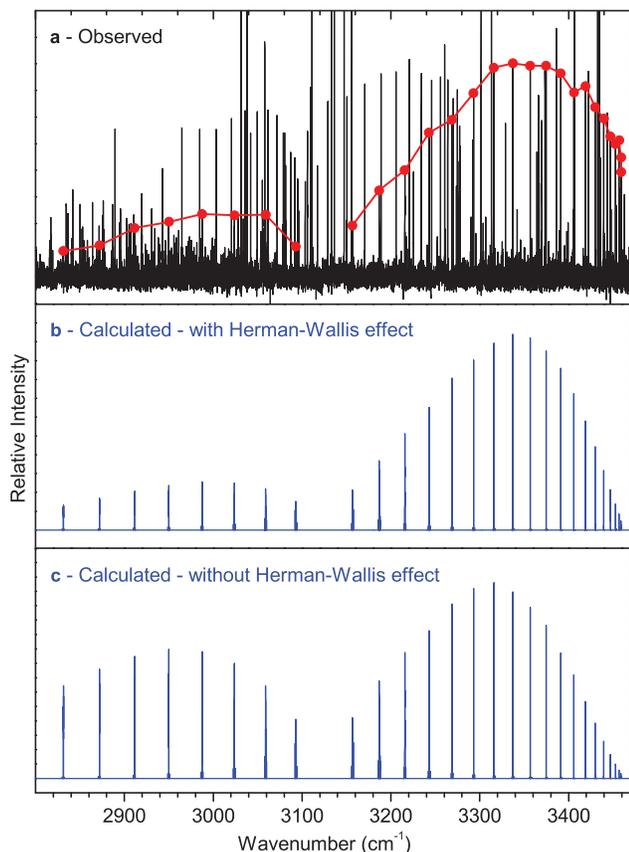
FIG. 5. Observed and calculated IR spectra of NH. (a) FTS spectrum obtained at Old Dominion University, Norfolk, VA. The red line and dots indicate the intensity of the 1-0 band P branch (left) and R branch (right). The lines that continue past the top of the y axis are intense atomic lines. The R branches of the 2-1, 3-2, and 4-3 bands are the other features that are clearly visible here. (b) and (c). Calculated spectra of the NH 1-0 band only, with and without the inclusion of the H-W effect. Its inclusion gives a better relative intensity difference between the P and R branches. The calculated spectrum was convolved with a Gaussian function to best match the observed broadening. A rotational temperature of 1300 K was used.

for I could be calculated. The resulting R/P ratios are also shown in Figure 4.

C. Lifetimes and band strengths

The experimental lifetime of the NH v = 1 level of Campbell *et al.*[19] of $37.0 \pm 0.5_{\text{stat}\,-0.8\text{syst}}^{\quad+2.0}$ ms matches very well with their calculated lifetime of 36.99 ms. We have calculated vibrational lifetimes using our final Einstein A values, by taking the reciprocal of the sum of the Einstein A values for all possible transitions from the same $N' = 0$, $J' = 1$ level. This results in a lifetime of 36.77 ms, which compares well to recent values of Campbell *et al.* Similarly, lifetimes of 17.09, 10.93, 8.10, 6.57, and 5.71 ms were calculated for v = 2-6, respectively.

Einstein $A_{v'v}$ values have been calculated for all reported vibrational bands, and the observed $\Delta v = 1$ sequence values are shown in Table IV, where disagreement with those of Dodd *et al.*[66] and Rosmus and Werner[67] is shown. These are calculated by summing over the Einstein A values for all possible transitions with $N' = 1$, $J' = 1$, for each band. The

TABLE IV. Einstein $A_{v'v}$ and $f_{v'v}$ values for vibrational transitions within the $X^3\Sigma^-$ state of NH, where $\Delta v = 1$.

	Einstein $A_{v'v}$ (s^{-1})				$f_{v'v}$
	Ours	D[a]	R&W[b]	M&R[c]	
1-0	27.19	51.7	34.9	31.69	3.941(-6)[d]
2-1	57.91	92.3		69.18	9.349(-6)
3-2	90.14	144.4		108.12	1.632(-5)
4-3	121.40			144.49	2.481(-5)
5-4	148.70			173.94	3.461(-5)
6-5	168.92			191.70	4.527(-5)

[a]Dodd *et al.*[66]
[b]Rosmus and Werner.[67]
[c]Our calculations repeated using the 1975 DMF of Meyer and Rosmus.[57]
[d]Numbers in parentheses indicate the exponent.

Einstein $A_{v'v}$ values have also been converted into vibrational band oscillator strengths ($f_{v'v}$-values) using the equation[88]

$$f_{v'v} = 1.49919368 \,\frac{1}{\bar{\nu}^2}\, \frac{(2 - \delta_{0,\Lambda'})}{(2 - \delta_{0,\Lambda})} A_{v'v}, \qquad (5)$$

where $\Lambda' = \Lambda'' = 0$. The full set of Einstein $A_{v'v}$ and $f_{v'v}$ values are available in Supplement 4 of the supplementary material.[71]

Our value for μ_0 of 1.5246 D compares well to the values of the theoretical studies shown in Table I (μ_e is also shown to enable comparison with all studies). However, it lies just outside the error bounds of the experimental value obtained by Scarl and Dalby in 1974.[52] As discussed above, our v = 1 lifetime shows excellent agreement with the experimental value measured recently by Campbell *et al.*[19] using magnetic trapping. Scarl and Dalby determined μ_0 from the Stark shift in the $A^3\Pi$-$X^3\Sigma^-$ transition, assuming that $\mu_0(A)$ = 1.3 D. We calculated $\mu_0(A)$ at the same level of theory as the ground state, and found a value of 1.412 D. If we adapt Eq. (10) of Ref. 52 by replacing 2.80 ± 0.13 in the numerator by $2.80 \times (1.412/1.3)^2$ we find $\mu_0(X) = 1.38 \ldots 1.52$ D, where the upper limit agrees with our *ab initio* value.

In 1989, Chackerian *et al.*[42] measured the Herman-Wallis effect from an observed spectrum and used this along with the value of μ_0 from Scarl and Dalby in their calculations of the matrix element $\langle v = 1|\mu|v = 0\rangle$. If, in their Eq. (3), all of the terms are replaced by our values ($\mu_0 = 1.52456$, ω_e and B_e from Table II, and $C_0^1 = 0.07895$), the result is -0.0559 D, which shows a much better match to our *ab initio* value of -0.05615 D.

D. Calculations with the 1975 Meyer and Rosmus dipole moment function

As the Meyer and Rosmus DMF from 1975[57] has previously been used to calculate NH rovibrational line intensities, the full set of calculations described in this paper were also performed with this DMF as a test. The resulting Einstein $A_{v'v}$ values can be seen in Table IV. This shows that even though the values of μ_e of the new DMF and the 1975 DMF only disagree by $\sim 3.5\%$, the differences between the full DMFs and the amount of extrapolation necessary cause the resulting line

intensities to disagree by a much greater percentage. The two DMFs are shown in Figure 1.

IV. CONCLUSION

Discrepancies have previously been seen in NH line strengths (see Secs. I and III C), and with the aim of helping to resolve them, a new dipole moment function for the $X^3\Sigma^-$ state of NH has been reported that we believe to be the most accurate to date. It has been used along with the data of Ram and Bernath[41] to calculate a new line list (see Supplement 5 of the supplementary material[71]) of rotational and rovibrational transitions, including line positions and intensities in the form of Einstein *A* values and *f*-values, taking the Herman-Wallis effect into account. This line list will be useful for the study of NH in astronomy, cold and ultracold molecular systems, and in the nitrogen chemistry of combustion.

ACKNOWLEDGMENTS

APPENDIX: DETAILS OF LINE INTENSITY CALCULATIONS

1. Transformation from Hund's case (b) to case (a) matrix elements

Please note that the matrix elements in this section are all for the ground electronic state. LEVEL does not include electron spin, and therefore its calculated TDMMEs are of the form

$$\langle v'\Lambda'N'|T_q^k|v\Lambda N\rangle, \tag{A1}$$

where k is the rank of the transition, and equal to 1 for single photon electric dipole transitions, and the component q is 0 for parallel and ± 1 for perpendicular transitions. The dependence on N of this quantity gives rise to the Herman-Wallis effect. Note that these are vibronic matrix elements, and exclude the angular dependence of the wavefunction (but do include the rotational dependence of the vibronic wavefunctions).

As the matrix elements in Eq. (A1) specify N, they can be used as is for a calculation in a Hund's case (b) basis. Although the NH $X^3\Sigma^-$ state is close to Hund's case (b), PGOPHER uses a Hund's case (a) basis set, and therefore the case (b) MEs from LEVEL need to be converted to case (a). This can also be considered as a transformation from spinless case (b) MEs to case (a) MEs that include spin.

The MEs can be transformed from Hund's case (b) to (a) using the equation

$$\langle v'\Lambda'J'\Omega'|T_q^k|v\Lambda J\Omega\rangle = (-1)^{J'-\Omega'}\begin{pmatrix} J' & k & J \\ -\Omega' & q & \Omega \end{pmatrix}^{-1}$$

$$\times \sum_{N,N'}(-1)^{N-N'+S+J+k+\Lambda}(2N+1)(2N'+1)\begin{pmatrix} J' & S & N' \\ \Omega' & -\Sigma & -\Lambda' \end{pmatrix}\begin{pmatrix} J & S & N \\ \Omega & -\Sigma & -\Lambda \end{pmatrix}$$

$$\times \begin{Bmatrix} N' & J' & S \\ J & N & k \end{Bmatrix}\begin{pmatrix} N' & k & N \\ -\Lambda' & q & \Lambda \end{pmatrix}\langle v'\Lambda'N'|T_q^k|v\Lambda N\rangle, \tag{A2}$$

which in this case is

$$\langle v'0J'\Omega'|T_0^1|v0J\Omega\rangle = (-1)^{J'-\Omega'}\begin{pmatrix} J' & 1 & J \\ -\Omega' & 0 & \Omega \end{pmatrix}^{-1}$$

$$\times \sum_{N,N'}(-1)^{N-N'+J+2}(2N+1)(2N'+1)\begin{pmatrix} J' & 1 & N' \\ \Omega' & -\Sigma & 0 \end{pmatrix}\begin{pmatrix} J & 1 & N \\ \Omega & -\Sigma & 0 \end{pmatrix}$$

$$\times \begin{Bmatrix} N' & J' & 1 \\ J & N & 1 \end{Bmatrix}\begin{pmatrix} N' & 1 & N \\ 0 & 0 & 0 \end{pmatrix}\langle v'0N'|T_0^1|v0N\rangle. \tag{A3}$$

This equation was derived mainly for use with the CN[37] and CP[87] $A^2\Pi$-$X^2\Sigma^+$ transitions, as the upper A state is case (a) for CP and a mixture of (a) and (b) for CN, and therefore transformation from the LEVEL case (b) MEs was important. However, it still has a small effect when the states involved are case (b) because of the use of the case (a) basis set by

PGOPHER, and so as the transformation was possible, it was also used for the $B^2\Sigma^+$-$X^2\Sigma^+$ transition and the $X^2\Sigma^+$ state rovibrational transitions of CN,[37] and it is used in the calculations in this paper for the same reason. The derivation was explained in detail in the supplementary material of Brooke *et al.*[37,89]

On the right-hand side of the equation, $\langle v'0N'|T_0^1|v0N\rangle$, is the Hund's case (b) ME that is calculated by LEVEL, which applies to a specific transition involving given values of N' and N''. The case (a) ME on the left-hand side specifies the transition in terms of J and Ω, and these are calculated by summing over all the case (b) MEs (specified in terms of N' and N'') that can contribute to the chosen $J'\Omega' - J''\Omega''$ transition. The numerical factors in the equation arise from the transformation between Hund's case (a) and (b) wavefunctions. The final result is that a case (a) ME is calculated from a weighted average of the contributing case (b) MEs. This is explained in more detail below.

For an $X^3\Sigma^-$ state, PGOPHER uses the Hund's case (a) basis states $|v J \Omega = +1\rangle$, $|v J \Omega = 0\rangle$, and $|v J \Omega = -1\rangle$. For the P and R branches (in terms of ΔJ), there are three non-zero MEs between these basis states: $\langle v' J' \Omega' = +1|T_0^1|v J \Omega = +1\rangle$, $\langle v' J' \Omega' = 0|T_0^1|v J \Omega = 0\rangle$, and $\langle v' J' \Omega' = -1|T_0^1|v J \Omega = -1\rangle$ (except for where J'' or J' are 0). For the Q branch, the non-zero MEs are $\langle v' J' \Omega' = +1|T_0^1|v J \Omega = +1\rangle$ and $\langle v' J' \Omega' = -1|T_0^1|v J \Omega = -1\rangle$. $\langle v' J' \Omega' = +1|T_0^1|v J \Omega = +1\rangle$ and $\langle v' J' \Omega' = -1|T_0^1|v J \Omega = -1\rangle$ are equal by symmetry, as they are invariant to reversal of the signs of all the projections ($\Lambda = 0$ and $\Sigma = \Omega$). Therefore, values must be calculated for five MEs for each lower J level: $\langle v' J' \Omega' = +1|T_0^1|v J \Omega = +1\rangle$ and $\langle v' J' \Omega' = 0|T_0^1|v J \Omega = 0\rangle$ for both the P and R branches, and $\langle v' J' \Omega' = +1|T_0^1|v J \Omega = +1\rangle$ for the Q branch. Values for these MEs for all required rotational transitions were calculated using Eq. (A3). The resulting case (a) MEs were set up in PGOPHER, which first transforms these pure omega MEs into symmetrized case (a) MEs, and then performs the diagonalization of the Hamiltonian in the symmetrized case (a) basis, resulting in a transformed transition matrix in terms of the true states. This is described in more detail in Sec. II.

The summation part of the equation is over all N'-N'' transitions that are possible for a particular J and Ω transition. For the R branch transitions (except for where J'' or J' are 0), there are four N transitions that contribute to the overall intensity. These are, for example, for the R(6) transition, $N' - N'' = $ 6-5, 6-7, 8-7, and 7-6. These are included in the summation part for the calculation of both the $\langle v' J' \Omega' = +1|T_0^1|v J \Omega = +1\rangle$ and $\langle v' J' \Omega' = 0|T_0^1|v J \Omega = 0\rangle$ MEs. Similarly, there are four N transitions for the P branch $\langle v' J' \Omega' = +1|T_0^1|v J \Omega = +1\rangle$ and $\langle v' J' \Omega' = 0|T_0^1|v J \Omega = 0\rangle$ MEs, and four for the Q branch ME.

2. Calculation of $S_{\eta'J'\eta J}$ from Hund's case (a) TDMMEs using PGOPHER

Please note that the matrix elements in this section are all for the ground electronic state. The line strength, $S_{\eta'J'\eta J}$ (in debye squared; where the electronic state, vibration, electron spin, and orbital angular momentum are included in η), is equal to the squared transition dipole moment summed over the degenerate M components of both states and the possible polarizations of the light,

$$S_{\eta'J'\eta J} = \Sigma_{p,M',M} |\langle v' J' M' N'|T_p^k(\mu)|v J M N\rangle|^2, \quad \text{(A4)}$$

TABLE V. Pure omega transition matrix set up by PGOPHER for the (1,0), R(4) example transition.

	$\langle v' \, J' \, \Omega' = +1|$	$\langle v' \, J' \, \Omega' = 0|$	$\langle v' \, J' \, \Omega' = -1|$
$|v \, J \, \Omega = +1\rangle$	-0.148373	0	0
$|v \, J \, \Omega = 0\rangle$	0	-0.151539	0
$|v \, J \, \Omega = -1\rangle$	0	0	-0.148373

which is equal to $|\langle v'J'N'|T^k(\mu)|v J N\rangle|^2$. Therefore there is one Eq. (A4) for each transition between the individual e and f parity levels.

To obtain these MEs, the Hund's case (a) MEs calculated as described in Sec. I must be converted to MEs in terms of the true fine structure states. For each J transition, a 3×3 pure omega transition matrix is set up by PGOPHER using the calculated case (a) vibrational MEs, $\langle v'0J'\Omega'|T_0^1|v0J\Omega\rangle$.

The matrix elements $\langle v'0J'\Omega'|T_0^1|v0J\Omega\rangle$ above exclude the required averaging over the angles between space and body fixed axis systems. The complete matrix element thus requires an additional factor:

$$(-1)^{J'-\Omega'}\sqrt{(2J'+1)(2J+1)}\begin{pmatrix} J' & 1 & J \\ -\Omega' & 0 & \Omega \end{pmatrix}. \quad \text{(A5)}$$

The pure omega matrix is transformed to a symmetrized matrix, with the basis functions:

$$|v J 0\rangle = |v \, J \, \Omega = 0\rangle, \quad \text{(A6)}$$

$$|v J +\rangle = \frac{|v \, J \, \Omega = +1\rangle + |v \, J \, \Omega = -1\rangle}{\sqrt{2}}, \quad \text{(A7)}$$

and

$$|v J -\rangle = \frac{|v \, J \, \Omega = +1\rangle - |v \, J \, \Omega = -1\rangle}{\sqrt{2}}. \quad \text{(A8)}$$

For the P and R branches, this results in one 2×2 and one 1×1 matrix, for the $|v J +\rangle/|v J 0\rangle$ and $|v J -\rangle$ basis functions, respectively. For example, for the (1,0), R(4) transition, the original and symmetrized matrices are shown in Tables V and VI, and the 1×1 matrix has the element $\langle v'J' - |T_0^1(\mu)|v J -\rangle = -0.148373$.

For the Q branch, it results in two 2×1 matrices, one where the basis functions are $\langle v'J' + |$, $\langle v'J'0|$ and $|v J -\rangle$, and one where they are $\langle v'J' - |$, $|v J +\rangle$ and $|v J 0\rangle$. These "original" transition matrices, **O**, are combined with the eigenvector matrices from the diagonalization of the Hamiltonian, giving the "transformed" transition matrices, **T**, in terms of the real F levels. For example, for the e parity (F_1 and F_3) transitions, **T** is obtained from

$$\mathbf{T} = \mathbf{X_l^T O X_u}, \quad \text{(A9)}$$

TABLE VI. Symmetrized e parity transition matrix calculated by PGOPHER for the (1,0), R(4) example transition.

	$\langle v'J' + |$	$\langle v'J'0|$
$|v J +\rangle$	-0.148373	0
$|v J 0\rangle$	0	-0.151539

TABLE VII. Transformed *e* parity transition matrix, **T**, calculated by PGOPHER for the (1,0), R(4) example transition, in terms of the true F levels.

	$\langle \eta' \, J' \, F' = 1 |$	$\langle \eta' \, J' \, F' = 2 |$
$| \eta \, J \, F = 1 \rangle$	-0.149798	0.000121
$| \eta \, J \, F = 2 \rangle$	$.003030$	-0.150099

where $\mathbf{X_u}$ and $\mathbf{X_l}$ are the upper and lower eigenvector matrices, respectively.

The *e* parity **T** matrix for (1,0), R(4) is shown in Table VII. These are the $|\langle v'J'N'|T^k(\mu)|vJN\rangle|^2$ MEs mentioned above, and so $S_{\eta'J'\eta J}$, and then the Einstein *A* values, can be calculated directly. For the example transition, $S_{\eta'J'\eta J}$ is equal to the values in Table VII squared, and the Einstein *A* values are 21.8182, 22.9405, .0067193, and 0.00001923 s^{-1} for the F_{11}, F_{33}, F_{13}, and F_{31} transitions, respectively.

[1] S. T. Ridgway and J. W. Brault, Ann. Rev. Astron. Astrophys. **22**, 291 (1984).
[2] P. F. Bernath, Int. Rev. Phys. Chem. **28**, 681 (2009).
[3] D. L. Lambert and R. Beer, Astrophys. J. **177**, 541 (1972).
[4] D. L. Lambert, J. A. Brown, K. H. Hinkle, and H. R. Johnson, Astrophys. J. **284**, 223 (1984).
[5] V. V. Smith and D. L. Lambert, Astrophys. J. **311**, 843 (1986).
[6] W. Aoki and T. Tsuji, Astron. Astrophys. **328**, 175 (1997).
[7] M. M. Litvak and E. N. R. Kuiper, Astrophys. J. **253**, 622 (1982).
[8] D. M. Meyer and K. C. Roth, Astrophys. J. Lett. **376**, L49 (1991).
[9] I. A. Crawford and D. A. Williams, Mon. Not. R. Astron. Soc. **291**, L53 (1997).
[10] J. R. Goicoechea, N. J. Rodríguez-Fernández, and J. Cernicharo, Astrophys. J. **600**, 214 (2004).
[11] T. Weselak, G. A. Galazutdinov, Y. Beletsky, and J. Krełowski, Mon. Not. R. Astron. Soc. **400**, 392 (2009).
[12] F. E. Roach, Astrophys. J. **89**, 99 (1939).
[13] C. B. Farmer and R. H. Norton, *A High-Resolution Atlas of the Infrared Spectrum of the Sun and the Earth Atmosphere from Space. A Compilation of ATMOS Spectra of the Region from 650 to 4800 cm^{-1} (2.3 to 16 µm). Vol. I. The Sun.* (NASA Langley Research Center, Hampton, VA, USA, 1989).
[14] N. Grevesse, D. L. Lambert, A. J. Sauval, E. F. van Dishoeck, C. B. Farmer, and R. H. Norton, Astron. Astrophys. **232**, 225 (1990).
[15] M. Geller, C. B. Farmer, R. H. Norton, A. J. Sauval, and N. Grevesse, Astron. Astrophys. **249**, 550 (1991).
[16] N. Grevesse, M. Asplund, and A. J. Sauval, Space Sci. Rev. **130**, 105 (2007).
[17] W. C. Campbell, E. Tsikata, H.-I. Lu, L. D. van Buuren, and J. M. Doyle, Phys. Rev. Lett. **98**, 213001 (2007).
[18] S. Hoekstra, M. Metsälä, P. C. Zieger, L. Scharfenberg, J. J. Gilijamse, G. Meijer, and S. Y. T. van de Meerakker, Phys. Rev. A **76**, 063408 (2007).
[19] W. C. Campbell, G. C. Groenenboom, H.-I. Lu, E. Tsikata, and J. M. Doyle, Phys. Rev. Lett. **100**, 083003 (2008).
[20] M. T. Hummon, W. C. Campbell, H.-I. Lu, E. Tsikata, Y. Wang, and J. M. Doyle, Phys. Rev. A **78**, 050702 (2008).
[21] M. Kajita, Phys. Rev. A **74**, 032710 (2006).
[22] L. M. C. Janssen, P. S. Żuchowski, A. van der Avoird, G. C. Groenenboom, and J. M. Hutson, Phys. Rev. A **83**, 022713 (2011).
[23] L. M. C. Janssen, P. S. Żuchowski, A. van der Avoird, J. M. Hutson, and G. C. Groenenboom, J. Chem. Phys. **134**, 124309 (2011).
[24] L. M. C. Janssen, A. van der Avoird, and G. C. Groenenboom, Eur. Phys. J. D **65**, 177 (2011).
[25] L. M. C. Janssen, A. van der Avoird, and G. C. Groenenboom, Phys. Rev. Lett. **110**, 063201 (2013).
[26] M. Kajita, Phys. Rev. A **74**, 035403 (2006).
[27] A. O. G. Wallis and J. M. Hutson, Phys. Rev. Lett. **103**, 183201 (2009).
[28] A. O. G. Wallis, E. J. J. Longdon, P. S. Żuchowski, and J. M. Hutson, Eur. Phys. J. D **65**, 151 (2011).
[29] H. L. Bethlem and W. Ubachs, Faraday Discuss. **142**, 25 (2009).
[30] D. Demille, Phys. Rev. Lett. **88**, 067901 (2002).
[31] J. A. Miller and C. T. Bowman, Prog. Energy Combust. Sci. **15**, 287 (1989).
[32] L. D. Smoot, S. C. Hill, and H. Xu, Prog. Energy Combust. Sci. **24**, 385 (1998).
[33] K. Lodders and B. Fegley, Jr., Icarus **155**, 393 (2002).
[34] J. I. Moses, C. Visscher, J. J. Fortney, A. P. Showman, N. K. Lewis, C. A. Griffith, S. J. Klippenstein, M. Shabram, A. J. Friedson, M. S. Marley, and R. S. Freedman, Astrophys. J. **737**, 15 (2011).
[35] D. L. Lambert, B. Gustafsson, K. Eriksson, and K. H. Hinkle, Astrophys. J. Suppl. Ser. **62**, 373 (1986).
[36] M. Asplund, N. Grevesse, A. J. Sauval, and P. Scott, Annu. Rev. Astron. Astrophys. **47**, 481 (2009).
[37] J. S. A. Brooke, R. S. Ram, C. M. Western, D. W. Schwenke, G. Li, and P. F. Bernath, Astrophys. J. Suppl. Ser. **210**, 23 (2014).
[38] P. F. Bernath and T. Amano, J. Mol. Spectrosc. **95**, 359 (1982).
[39] D. Boudjaadar, J. Brion, P. Chollet, G. Guelachvili, and M. Vervloet, J. Mol. Spectrosc. **119**, 352 (1986).
[40] R. S. Ram, P. F. Bernath, and K. H. Hinkle, J. Chem. Phys. **110**, 5557 (1999).
[41] R. S. Ram and P. F. Bernath, J. Mol. Spectrosc. **260**, 115 (2010).
[42] C. Chackerian, Jr., G. Guelachvili, A. López-Piñeiro, and R. H. Tipping, J. Chem. Phys. **90**, 641 (1989).
[43] H. E. Radford and M. M. Litvak, Chem. Phys. Lett. **34**, 561 (1975).
[44] F. D. Wayne and H. E. Radford, Mol. Phys. **32**, 1407 (1976).
[45] F. C. van den Heuvel, W. L. Meerts, and A. Dymanus, Chem. Phys. Lett. **92**, 215 (1982).
[46] P. F. Bernath, C. T. McElroy, M. C. Abrams, C. D. Boone, M. Butler, C. Camy-Peyret, M. Carleer, C. Clerbaux, P.-F. Coheur, R. Colin, P. DeCola, M. DeMazière, J. R. Drummond, D. Dufour, W. F. J. Evans, H. Fast, D. Fussen, K. Gilbert, D. E. Jennings, E. J. Llewellyn, R. P. Lowe, E. Mahieu, J. C. McConnell, M. McHugh, S. D. McLeod, R. Michaud, C. Midwinter, R. Nassar, F. Nichitiu, C. Nowlan, C. P. Rinsland, Y. J. Rochon, N. Rowlands, K. Semeniuk, P. Simon, R. Skelton, J. J. Sloan, M.-A. Soucy, K. Strong, P. Tremblay, D. Turnbull, K. A. Walker, I. Walkty, D. A. Wardle, V. Wehrle, R. Zander, and J. Zou, Geophys. Res. Lett. **32**, L15S01, doi:10.1029/2005GL022386 (2005).
[47] F. Hase, L. Wallace, S. D. McLeod, J. J. Harrison, and P. F. Bernath, J. Quant. Spectrosc. Radiat. Transfer **111**, 521 (2010).
[48] T. Klaus, S. Takano, and G. Winnewisser, Astron. Astrophys. **322**, L1 (1997).
[49] F. Lewen, S. Brünken, G. Winnewisser, M. Šimečková, and Š. Urban, J. Mol. Spectrosc. **226**, 113 (2004).
[50] J. Flores-Mijangos, J. M. Brown, F. Matsushima, H. Odashima, K. Takagi, L. R. Zink, and K. M. Evenson, J. Mol. Spectrosc. **225**, 189 (2004).
[51] A. Robinson, J. M. Brown, J. Flores-Mijangos, L. Zink, and M. Jackson, Mol. Phys. **105**, 639 (2007).
[52] E. A. Scarl and F. W. Dalby, Can. J. Phys. **52**, 1429 (1974).
[53] J. S. Muenter, J. Mol. Spectrosc. **55**, 490 (1975).
[54] D. Feller and J. A. Sordo, J. Chem. Phys. **112**, 5604 (2000).
[55] B. Temelso, E. F. Valeev, and C. D. Sherrill, J. Phys. Chem. A **108**, 3068 (2004).
[56] G. Das, A. C. Wahl, and W. J. Stevens, J. Chem. Phys. **61**, 433 (1974).
[57] W. Meyer and P. Rosmus, J. Chem. Phys. **63**, 2356 (1975).
[58] P. J. Hay and T. H. Dunning, Jr., J. Chem. Phys. **64**, 5077 (1976).
[59] E. M. Goldfield and K. P. Kirby, J. Chem. Phys. **87**, 3986 (1987).
[60] J. R. Stallcop, C. W. Bauschlicher, Jr., H. Partridge, S. R. Langhoff, and E. Levin, J. Chem. Phys. **97**, 5578 (1992).
[61] E. Cantarella, F. Colot, and J. Liévin, Phys. Scr. **46**, 489 (1992).
[62] J. Paldus and X. Z. Li, Can. J. Chem. **74**, 918 (1996).
[63] H. M. Pickett, R. L. Poynter, E. A. Cohen, M. L. Delitsky, J. C. Pearson, and H. S. P. Müller, J. Quant. Spectrosc. Radiat. Transfer **60**, 883 (1998).
[64] H. S. P. Müller, S. Thorwirth, D. A. Roth, and G. Winnewisser, Astron. Astrophys. **370**, L49 (2001).
[65] H. S. P. Müller, F. Schlöder, J. Stutzki, and G. Winnewisser, J. Mol. Struct. **742**, 215 (2005).
[66] J. A. Dodd, S. J. Lipson, D. J. Flanagan, W. A. M. Blumberg, J. C. Person, and B. D. Green, J. Chem. Phys. **94**, 4301 (1991).
[67] P. Rosmus and H.-J. Werner, J. Mol. Struct. **60**, 405 (1980).
[68] P. F. Bernath, *Spectra of Atoms and Molecules*, 2nd ed. (Oxford University Press, 2005).
[69] C. M. Western, PGOPHER, a program for simulating rotational structure (v. 8.0.102), 2013.

[70] R. J. Le Roy, "LEVEL 8.0: A computer program for solving the radial Schrödinger equation for bound and quasibound levels," University of Waterloo Chemical Physics Research Report (University of Waterloo, 2007).

[71] See supplementary material at http://dx.doi.org/10.1063/1.4891468 for: 1. Hund's case (b) matrix elements (level .8 output), 2. RKR Potential energy curve and its interpolation/extrapolation by level, 3. *ab initio* potential and DMF, 4. line list including positions and intensities for rovibrational and rotational transitions, and 5. $A_{v'v}$ and $f_{v'v}$ values.

[72] R. J. Le Roy, "RKR1 2.0: A computer program implementing the first-order RKR method for determining diatomic molecule potential energy functions," University of Waterloo Chemical Physics Research Report (University of Waterloo, 2004).

[73] R. Rydberg, Z. Phys. **73**, 376 (1932).

[74] R. Rydberg, Z. Phys. **80**, 514 (1933).

[75] O. Klein, Z. Phys. **76**, 226 (1932).

[76] A. L. G. Rees, Proc. Phys. Soc. **59**, 998 (1947).

[77] J. Espinosa-García, J. C. Corchado, J. Fernández, and A. Marquez, Chem. Phys. Lett. **233**, 220 (1995).

[78] C. R. Brazier, R. S. Ram, and P. F. Bernath, J. Mol. Spectrosc. **120**, 381 (1986).

[79] H.-J. Werner and P. J. Knowles, J. Chem. Phys. **89**, 5803 (1988).

[80] P. J. Knowles and H.-J. Werner, Chem. Phys. Lett. **145**, 514 (1988).

[81] H.-J. Werner, P. J. Knowles, R. Lindh, F. R. Manby, M. Schütz *et al.*, MOLPRO, version 2006.1, a package of *ab initio* programs, 2006, see http://www.molpro.net.

[82] T. H. Dunning, Jr., J. Chem. Phys. **90**, 1007 (1989).

[83] D. E. Woon and T. H. Dunning, Jr., J. Chem. Phys. **103**, 4572 (1995).

[84] A. K. Wilson, T. van Mourik, and T. H. Dunning, Jr., J. Mol. Struct.: THEOCHEM **388**, 339 (1996).

[85] R. Herman and R. F. Wallis, J. Chem. Phys. **23**, 637 (1955).

[86] R. J. Le Roy and E. R. Vrscay, Can. J. Phys. **53**, 1560 (1975).

[87] R. S. Ram, J. S. A. Brooke, C. M. Western, and P. F. Bernath, J. Quant. Spectrosc. Radiat. Transfer **138**, 107 (2014).

[88] M. Larsson, Astron. Astrophys. **128**, 291 (1983).

[89] J. Brown and A. Carrington, *Rotational Spectroscopy of Diatomic Molecules*, Cambridge Molecular Science (Cambridge University Press, 2003).